NASA MEMO 1-30-59L

NASA

MEMORANDUM

EFFECTS OF CROSS-SECTIONAL SHAPE, SOLIDITY, AND DISTRIBUTION OF HEAT-TRANSFER COEFFICIENT ON THE TORSIONAL STIFFNESS OF THIN WINGS SUBJECTED TO AERODYNAMIC HEATING

By Robert G. Thomson

Langley Research Center
Langley Field, Va.

NATIONAL AERONAUTICS AND SPACE ADMINISTRATION

WASHINGTON
February 1959

NATIONAL AERONAUTICS AND SPACE ADMINISTRATION

MEMORANDUM 1-30-59L

EFFECTS OF CROSS-SECTIONAL SHAPE, SOLIDITY, AND DISTRIBUTION OF HEAT-TRANSFER COEFFICIENT ON THE TORSIONAL STIFFNESS OF THIN WINGS SUBJECTED TO AERODYNAMIC HEATING

By Robert G. Thomson

SUMMARY

A study has been made of the effects of varying the shape, solidity, and heat-transfer coefficient of thin wings with regard to their influence on the torsional-stiffness reduction induced by aerodynamic heating. The variations in airfoil shape include blunting, flattening, and combined blunting and flattening of a solid wing of symmetrical double-wedge cross section. Hollow double-wedge wings of constant skin thickness with and without internal webs also are considered. The effects of heat-transfer coefficients appropriate for laminar and turbulent flow are investigated in addition to a step transition along the chord from a lower to a higher constant value of heat-transfer coefficient. From the results given it is concluded that the flattening of a solid double wedge decreases the reduction in torsional stiffness while slight degrees of blunting increase the loss. The influence of chordwise variations in heat-transfer coefficient due to turbulent and laminar boundary-layer flow on the torsional stiffness of solid wings is negligible. The effect of a step transition in heat-transfer coefficient along the chord of a solid wing can, however, become appreciable. The torsional-stiffness reduction of multiweb and hollow double-wedge wings is substantially less than that calculated for a solid wing subjected to the same heating conditions.

INTRODUCTION

The influence of aerodynamic heating on the effective torsional stiffness of thin wings was investigated in reference 1. From the results presented, the loss of torsional stiffness in thin wings, rapidly accelerated to supersonic speeds, was found to be significant. This conclusion was based on calculations for a solid airfoil of double-wedge cross section with a constant heat-transfer coefficient. A hollow double-wedge

wing of constant skin thickness with a variable heat-transfer coefficient was also investigated. The magnitude of the loss in torsional stiffness was found to depend primarily on the chordwise mass variation of the airfoil cross section.

In the present paper the influence on torsional-stiffness reduction of changes in the mass and temperature distributions of the airfoil cross section is studied. The changes in the mass distribution were effected in two ways: By considering various modifications of a solid double-wedge cross section, and by considering an airfoil of multiweb construction. The changes in the temperature distribution (other than those which accompanied the change in the mass distribution) were effected by varying the heat-transfer coefficients. The effects of heat-transfer coefficients appropriate for laminar and turbulent flow were investigated in addition to a step transition along the chord from a lower to a higher constant heat-transfer coefficient. Details of the analyses are given in the appendixes.

SYMBOLS

A	cross-sectional area
a	semiwidth of flat portion of modified wedge
B	arbitrary constant
b	modified wedge dimension (see fig. 1)
b_w	web spacing
c	chord
c_m	specific heat of wing material
d	distance from leading edge of wing
E	Young's modulus
G	shear modulus
h	heat-transfer coefficient
I	moment of inertia
J	torsional-stiffness constant
K	constant

k_a thermal conductivity of air

$L = a + b - \frac{c}{2}$

M Mach number

N_{Pr} Prandtl number

R Reynolds number

T average temperature through thickness of wing

ΔT_{aw} difference between initial and final adiabatic wall temperature

t wing thickness

x distance from midchord of cross section

α coefficient of thermal expansion

β dummy variable

γ ratio of specific heats

ϵ spanwise strain

η_r temperature-recovery factor

θ temperature parameter, $\frac{T - T_o}{\Delta T_{aw}}$

λ time parameter

$\xi = \frac{2d}{c}$

ρ mass density of wing material

σ normal stress in spanwise direction

τ time

Φ torsional-stiffness-reduction parameter (see eq. (12))

Subscripts:

av	average
aw	adiabatic wall condition
c/2	at midchord
eff	effective
f	final
lam	laminar
le	leading edge
max	maximum
o	initial flight condition
s	skin
t	total
te	trailing edge
turb	turbulent
w	web
∞	free stream

BASIC THEORY

The torsional behavior of thin wings can be strongly influenced by the presence of axial stresses. An expression for the effective torsional stiffness GJ_{eff} of a thin wing of arbitrary cross section subjected to axial stresses has been derived in reference 1 and is

$$\frac{GJ_{eff}}{GJ_o} = 1 + \int_A \frac{\sigma r^2 dA}{G\Gamma_o} \tag{1}$$

where

GJ_o initial torsional stiffness

σ spanwise normal stress (tension positive)

r distance from axis of twist to point in question

When the wing is accelerated to supersonic speeds aerodynamic heating induces spanwise thermal stresses in the wing structure which in turn cause a change in the torsional stiffness as shown in equation (1). The seriousness of this change depends on a variety of factors such as flight condition, heat-transfer coefficient, mass distribution, and the thermal properties of the wing material.

Temperature Equations

In order to determine the chordwise temperature distribution (and consequently the spanwise stress) in a wing accelerated to supersonic speeds, the following assumptions are made:

The wing is assumed to be instantaneously accelerated from an initial Mach number M_o to a final Mach number M_f at a constant altitude. This assumption is based on the conclusions reached in reference 1 that the maximum loss of torsional stiffness for moderately rapid accelerations is only slightly less than that calculated for instantaneous acceleration. The local free-stream temperature and Mach number are taken to be those of the free stream ahead of the wing. Thus, the free-stream temperature is constant throughout the flight and the heat-transfer coefficient h is not a function of time. The heat-transfer coefficient is considered to be symmetric about the chordline corresponding to a 0^o angle of attack.

The initial wing temperature at time zero is assumed to be uniform and equal to the adiabatic wall temperature at the initial free-stream Mach number M_o. The adiabatic wall temperature is given by

$$T_{aw} = T_\infty\left[1 + \frac{\eta_r(\gamma - 1)M^2}{2}\right] \tag{2}$$

where

T_∞ local free-stream temperature

η_r temperature-recovery factor

Chordwise and spanwise heat conduction, as well as radiation effects, are neglected. Thus, a heat balance equation governing the chordwise temperature distribution can be expressed in terms of the average temperature through the thickness as

$$h\left(T_{aw} - T\right) = \rho c_m \frac{t}{2} \frac{\partial T}{\partial \tau} \tag{3}$$

where

T average temperature through thickness of wing

τ time

ρ mass density of wing material

c_m specific heat of wing material

t wing thickness

Consequently, the average temperature at any point along the chord can be expressed in nondimensional form as a function of a time parameter λ and a ratio of wing thickness to thickness at the midchord $\frac{t}{t_{max}}$ as

$$\theta = \frac{T - T_o}{\Delta T_{aw}} = 1 - e^{\frac{-\lambda}{t/t_{max}}} \tag{4}$$

where

T_o initial wing temperature

ΔT_{aw} difference between initial and final adiabatic wall temperature

and

$$\lambda = \frac{2h\tau}{\rho c_m t_{max}} \tag{5}$$

From equation (5) it can be seen that for constant values of ρ, c_m, and t_{max} the chordwise variation of λ is proportional to the chordwise variation of h, which in turn is dependent mainly on the condition of the fluid flow over the airfoil surface.

Heat-Transfer Coefficients

In order to study the influence of a variation in heat-transfer coefficient along the chordlength on the stiffness reduction, heat-transfer coefficients appropriate for turbulent and laminar boundary-layer flow need to be considered. For this analysis, flat-plate heat-transfer coefficients are assumed, and the Mach number on all surfaces is assumed to be the same as that of the free stream ahead of the wing.

For the case of turbulent boundary-layer flow, the heat-transfer coefficient at a point can be expressed by the empirical equation given in reference 2 as

$$h_{turb} = \frac{0.029 k_a R_d^{4/5} N_{Pr}^{1/3}}{d} \tag{6}$$

where d is the distance from the leading edge to the point in question. By using the known identities for Mach number and Reynolds number, equation (6) can be rewritten in terms of $d^{-1/5}$ and may be expressed in terms of the heat-transfer coefficient at the midchord as

$$h_{turb} = \frac{h_{turb,c/2}}{\left(\frac{2d}{c}\right)^{1/5}} \tag{7}$$

Similarly, if the flow is laminar the heat-transfer coefficient can be obtained by the use of the empirical equation given in reference 2 and is expressed as

$$h_{lam} = \frac{0.33 k_a R_d^{1/2} N_{Pr}^{1/3}}{d} \tag{8}$$

Equation (8) can also be rewritten in terms of the heat-transfer coefficient at the midchord as

$$h_{lam} = \frac{h_{lam,c/2}}{\left(\frac{2d}{c}\right)^{1/2}} \tag{9}$$

Thermal-Stress Equations

Once the heat-transfer coefficient is established and the temperature distribution is known, the thermal stresses can be calculated on

the basis of elementary beam theory in which it is assumed that plane sections remain plane with no lateral restraint. The material properties are considered to be invariant with temperature and all deformations are assumed to be elastic.

Since the doubly symmetric sections considered in this paper can undergo only a chordwise rotation and translation of the cross section, the spanwise strain can be written as

$$\epsilon = K + Bx = \frac{\sigma}{E} + \alpha(T - T_o) \tag{10}$$

where K and B are constants.

Application of the equilibrium conditions of zero thrust and zero moment permits the evaluation of K and B in equation (10). The resulting expression for the spanwise stress can be written as

$$\frac{\sigma}{E\alpha\Delta T_{aw}} = \theta_{av} + x \frac{\int_A \theta x \, dA}{\int_A x^2 \, dA} - \theta \tag{11}$$

where

$$\theta_{av} = \frac{\int_A \theta \, dA}{A_t}$$

When the spanwise stresses on a free-end beam are due to temperature they are necessarily self-equilibrating and consequently the magnitude of the thermal-stress torque given in equation (1) $\left(\int_A \sigma r^2 \, dA\right)$ is independent of the axis of twist. For the doubly symmetric sections considered in this paper, however, the axis of twist is at the midchord of the cross section and for thin wings r may be approximated by x.

By substituting equations (4) and (11) into equation (1) and performing the necessary integrations, the change in torsional stiffness can be expressed as

$$\frac{GJ_{eff}}{GJ_o} = 1 - \frac{E\alpha}{G} \Delta T_{aw} \left(\frac{c}{\epsilon_{max}}\right)^2 \Phi \tag{12}$$

where the parameter Φ is a function of the time parameter λ and the shape of the cross section, but it is not a function of the thickness ratio $\frac{t_{max}}{c}$.

Since the thickness ratio $\frac{t_{max}}{c}$, material properties, and change in adiabatic wall temperature ΔT_{aw} are constant for an airfoil at a given flight condition, the percent reduction in torsional stiffness will depend solely on the magnitude of Φ. Furthermore, values of Φ may be compared directly for each of the examples to be considered in the following sections of the paper. The influence of varying the shape and solidity of the cross section and of the distribution of the heat-transfer coefficient on the percent reduction in torsional stiffness will therefore be determined by investigating the change in Φ.

ANALYSIS

Effect of Variations in Cross-Sectional Shape

In order to study the effects of varying the airfoil shape on the reduction of torsional stiffness in solid cross sections, the modified double-wedge wing shown in figure 1 was analyzed. The analysis was based on the assumption that the heat-transfer coefficient remained constant across the chord, and therefore λ in equation (5) is a function of time alone.

The temperature distribution and the thermal stress distribution are symmetric about the midchord and only a translation of the cross section can occur (i.e., $B = 0$ in equation (10) and $\int_A \theta x \, dA = 0$ in equation (11)). Expressions for the temperature and stress distributions over the cross section and the percent of torsional-stiffness reduction for the modified double-wedge wing are derived in appendix A.

In order to show the quantitative effects of flattening and blunting of a cross section on the torsional-stiffness reduction, the parameter Φ was evaluated for different degrees of flattening $\frac{a}{c}$ and blunting $\frac{t_{le}}{t_{max}}$ over short time intervals. The results are shown in figures 2 to 5.

The influence of the flattening only of a solid double-wedge cross section $\frac{t_{le}}{t_{max}} = 0$ on the torsional-stiffness reduction is shown in

figure 2. The stiffness parameter is plotted as a function of the time parameter λ for various degrees of flattening, ranging from the unmodified double-wedge $\left(\frac{a}{c} = 0\right)$ to the flat plate $\left(\frac{a}{c} = \frac{1}{2}\right)$. The curve for $\frac{a}{c} = 0$ is identical to that given in reference 1. In the limiting case of $\frac{a}{c} = \frac{1}{2}$ the wedge becomes a flat plate and, as would be expected, the reduction in torsional stiffness is zero. It is evident from figure 2 that flattening of a solid double wedge reduces the loss of torsional stiffness caused by aerodynamic heating. The greatest loss in torsional stiffness $(\Phi = 0.0456)$ occurred for the unmodified double wedge. As shown in reference 1 this value of Φ would correspond to a 50-percent reduction in torsional stiffness for a 5-percent-thick stainless-steel wing accelerated instantaneously from a Mach number of 0 to a Mach number of 4 at an altitude of 50,000 feet.

The influence of the blunting of a solid double-wedge cross section on the torsional-stiffness reduction can be studied by considering the flattened portion of the modified wing a/c to be equal to zero. In figure 3, Φ is plotted as a function of λ for various degrees of blunting. The degree of blunting is given by the ratio of tip thickness t_{le} to midchord thickness t_{max}. When $\frac{t_{le}}{t_{max}} = 0$, the reduction in torsional stiffness is identical to that calculated for a solid double wedge $\left(\frac{a}{c} = 0 \text{ in fig. 2}\right)$. As $\frac{t_{le}}{t_{max}}$ approaches unity the double wedge becomes a flat plate and the torsional-stiffness-reduction parameter Φ approaches zero. For a slight degree of blunting, however, there is an increase in the maximum value of Φ. In order to obtain a clearer picture of this variation, the maximum values of Φ were plotted as a function of the blunting ratio $\frac{t_{le}}{t_{max}}$ in figure 4. It is evident from figure 4 that for slight degrees of blunting, the maximum torsional-stiffness reduction is greater than that obtained using the unblunted double wedge. This increase in stiffness loss reaches a maximum of 11 percent for a blunting ratio of approximately 0.10. Blunting ratios greater than 0.20 are needed to decrease the maximum torsional-stiffness loss below that calculated for the unblunted wedge.

In figure 5 the effect of combined blunting and flattening of a solid double-wedge section is shown. The stiffness-reduction parameter Φ is plotted as a function of λ for various degrees of blunting $\frac{t_{le}}{t_{max}}$ of the leading and trailing edges of a flattened wedge where $a/c = 1/4$. The maximum reduction in torsional stiffness as a function

of the blunting ratio $\frac{t_{le}}{t_{max}}$ is plotted in figure 4. In this figure the maximum stiffness reduction for the blunted and flattened double wedge can be seen to be similar to that of the blunted wedge. The effect of flattening of the midchord, however, reduces the magnitude of the maximum stiffness reduction by approximately 50 percent in comparison with the blunted wedge.

Effect of Variations in Solidity

In order to investigate the effects of variations in solidity on the reduction of torsional stiffness, a wing of multiweb construction such as that shown in figure 6 was considered. The results of an analysis of the torsional-stiffness reduction due to aerodynamic heating of such a multiweb wing were presented in reference 3 for a constant heat-transfer coefficient. The analysis, however, was based on the assumption that the temperature of the webs remained unchanged while the temperature of the skins asymptotically approached the adiabatic wall temperature. Thus, the temperature gradient and consequently the thermal stresses of the cross section continue to increase to an asymptotic value since the alleviating effect of heat conduction between skin and webs is not present.

In the present analysis, the heat-transfer coefficient was considered constant, but in order to allow the temperature of the skin and web material eventually to equalize, the webs were allowed to absorb heat. The temperature of each skin was considered to vary as that of a flat plate and can be written as

$$\theta_s = 1 - e^{\frac{-\lambda}{2t_s/t_{max}}} \tag{13}$$

The temperature of the web material was considered to vary as if the web mass completely filled the multiweb and formed a solid double wedge. The temperature of individual webs is then established as the temperature of different chordwise locations on a solid double wedge so that

$$\theta_w = 1 - e^{\frac{-\lambda}{t/t_{max}}} \tag{14}$$

The average temperature in a typical bay of the multiweb can be expressed as

$$\theta = \frac{2b_w t_s \theta_s + t t_w \theta_w}{2b_w t_s + t t_w} \tag{15}$$

In order to evaluate the spanwise stress at any point along the chord the total area of the web material is considered to vary continuously along the chord in proportion to the wing thickness. The expression for θ in equation (15) can then be substituted into equation (11) for spanwise stress. Because of the symmetry of the temperature distribution about the midchord, $\int_A \theta x \, dA$ in equation (11) is equal to zero.

The expression for the torsional-stiffness-reduction parameter Φ of the multiweb is obtained in appendix B. In this analysis the torsional constant J_o was calculated on the basis that the webs were rigid in shear.

In figure 7 Φ is plotted as a function of λ for various ratios of skin thickness to maximum chord depth and ratios of web area to skin area A_w/A_s. For a specific ratio of A_w/A_s the maximum stiffness reduction increases with a decrease in the ratio of $\frac{t_s}{t_{max}}$, whereas for a specific ratio of $\frac{t_s}{t_{max}}$, the maximum stiffness reduction decreases with a decrease in A_w/A_s. When t_w approaches zero the multiweb reduces to a hollow double wedge and the drop in torsional stiffness becomes zero. Note that the maximum value of Φ is somewhat lower than that calculated for a solid double wedge.

In figure 8 a comparison between the torsional-stiffness reduction obtained from the present analysis and that obtained from the analysis based on the assumption of no heat conduction (ref. 3) into the webs is made for two multiweb wings. The wings are assumed to be instantaneously accelerated from an initial Mach number of 0.75 to a final Mach number of 4.0 at an altitude of 50,000 feet. For both wings $\frac{t_{max}}{c}$ and the web area to cover area A_w/A_s are taken to be, respectively, 0.03 and 0.35. The skin thickness t_s and ratio of web thickness to web spacing $\frac{t_w}{b_w}$, however, is varied from one wing to the other.

The solutions are initially in agreement, but when the webs absorb a sufficient amount of heat to decrease appreciably the temperature gradient between the skin and webs, the two solutions diverge. The torsional stiffness, as obtained from the present analysis, reaches a minimum. On the other hand, the torsional stiffness reduction obtained from the solution permitting no heat transfer to the webs continues to decrease and approaches an asymptotic value as the skin temperature approaches the adiabatic wall temperature.

In evaluating the constant heat-transfer coefficient, the value of h at the midchord ($d = c/2$) was chosen as reference and evaluated by the use of equation (6) for turbulent flow. The following values corresponding to an altitude of 50,000 feet were used in the calculations: The velocity of sound was taken to be 971 ft/sec; the kinematic viscosity was assumed to be 8.18×10^{-4} sq ft/sec; $k_a = 3.16 \times 10^{-6}$ Btu/ft-sec-^{o}F; and $N_{Pr}^{1/3} = 0.9$. The value of $c_m\rho$ for stainless steel was taken as 59.1 Btu/ft^3-^{o}F.

Effect of Variations in Heat-Transfer Coefficient

Effect of turbulent and laminar boundary-layer flow.- In the previous section the heat-transfer coefficient was assumed constant along the chord. Heat-transfer coefficients under actual flight conditions, however, vary along the chord as can be seen from reference 2. In order to study the effects of a variation in heat-transfer coefficient on the reduction in torsional stiffness, h was assumed to vary continuously across the chord in the manner given by equations (7) and (9) for turbulent and laminar boundary-layer flow. In equations (7) and (9) h was expressed in terms of the heat-transfer coefficient at the midchord in order to obtain a reference for comparison purposes. Inasmuch as the heat-transfer coefficients are nonsymmetrical about the midchord, the temperature distributions are no longer symmetric and consequently both a translation and a rotation of the cross section is possible. Furthermore, with the heat-transfer coefficient a function of chordwise position, an analytic solution for the torsional-stiffness parameter Φ is rather difficult to obtain. For the present analysis a numerical integration procedure described in appendix C was employed. This procedure was used to obtain the reduction in torsional stiffness for two specific wing configurations subjected to variable heat-transfer coefficients across the chord. The results are presented in figures 9 and 10.

In figure 9 the reduction in torsional stiffness of a solid double-wedge wing in turbulent and laminar boundary-layer flow is shown. For the sake of comparison the curve of torsional-stiffness reduction for a constant value of h is also presented. In the calculations of these results 20 chordwise stations were used. This number of stations was necessary to give accuracy within 1 percent when the calculations were compared with the analytical solution presented for a constant value of h in reference 1.

As shown in figure 9, the variation of heat-transfer coefficient does not substantially influence the magnitude of the torsional-stiffness reduction. The percent difference between Φ calculated for a variable and for a constant heat-transfer coefficient is 7 percent for laminar

flow and only 3 percent for turbulent flow. Thus, the stiffness reductions due to varying the heat-transfer coefficient are but a small percentage of the stiffness loss resulting from the mass distribution.

In figure 10 results are presented for the reduction in torsional stiffness of a hollow double-wedge airfoil in turbulent and laminar boundary-layer flow. For the hollow double wedge of constant skin thickness the reduction in torsional stiffness is due solely to chordwise variations of h. In the calculations of these results 40 chordwise stations were used. This number of stations was necessary to give accuracy within 1 percent when the calculations were compared with an exact solution derived in reference 1 for turbulent flow over a hollow double-wedge cross section. Note that the maximum value of Φ calculated for the hollow double wedge with laminar boundary-layer flow is only 38 percent of that calculated for a solid double wedge.

Effect of a step transition in heat-transfer coefficient.- In order to investigate the effect on stiffness reduction of a transition in heat-transfer coefficient along the chord a simplified approach to the problem has been made. The heat-transfer coefficient is assumed to vary as a step function along the chord. Because of the difficulty in obtaining an analytic solution, numerical integration procedures described in appendix C were employed. Calculated results are presented for step transitions at the midchord and quarterchord of a solid double-wedge section. From a comparison of the results obtained by the numerical procedure and those obtained by an analytic solution derived for a step transition at the midchord, it was found that 20 chordwise stations were sufficient to give agreement within 2 percent.

For a step transition at the midchord, the average temperature at any point along the chord can be expressed by

$$\left.\begin{aligned} \theta &= 1 - e^{\frac{-\lambda C}{1+(2x/c)}} \qquad (-c/2 \leqq x < 0) \\ \theta &= 1 - e^{\frac{-\lambda}{1-(2x/c)}} \qquad (0 < x \leqq c/2) \end{aligned}\right\} \tag{22}$$

where

$$C = \frac{h_{1e}}{h_{te}} = \text{Constant} \tag{23}$$

$$\lambda = \frac{2h_{te}\tau}{c_m \rho t_{max}} \tag{24}$$

For a step transition at the quarterchord, the average temperature at any point along the chord is written as

$$\left.\begin{aligned} \theta &= 1 - e^{\frac{-\lambda C}{1+(2x/c)}} \qquad (-c/2 \leqq x < -c/4) \\ \theta &= 1 - e^{\frac{-\lambda}{1+(2x/c)}} \qquad (-c/4 < x < 0) \\ \theta &= 1 - e^{\frac{-\lambda}{1-(2x/c)}} \qquad (0 < x \leqq c/2) \end{aligned}\right\} \quad (25)$$

The thermal stresses and torsional stiffness reductions are evaluated from the general derivation given in appendix C.

In figure 11 Φ is plotted as a function of λ for a step transition at the midchord for several different ratios of heat-transfer coefficient. For all the cases presented, the heat-transfer coefficient in the rearward portion remains the same and λ is evaluated using this heat-transfer coefficient. The maximum stiffness reduction occurs in the limiting case where the heat-transfer coefficient is of constant magnitude across the entire chord ($C = 1$). For progressive reductions in the leading-edge heat-transfer coefficient, the reduction in torsional stiffness decreases.

The effect of varying the point of transition along the chord is shown in figure 12 for a ratio of $h_{le}/h_{te} = 1/5$. The transition point is moved from the leading edge, to the quarterchord, to the midchord. For the three transition points considered, the smallest reduction in torsional stiffness occurs with the step transition at the quarterchord while the leading-edge position results in the greatest reduction.

CONCLUDING REMARKS

The distribution of the heat-absorbing mass of an airfoil cross section is the primary factor in determining the reduction in torsional stiffness induced by aerodynamic heating.

The percent reduction in torsional stiffness in a hollow double-wedge section, which is due entirely to the chordwise variation in heat-transfer coefficient caused by laminar and turbulent flow, is much smaller in magnitude than that calculated for a solid double wedge.

Calculations based on the solid double wedge indicate that the variation in heat-transfer coefficient due to turbulent and laminar boundary-layer flow had very little effect on the magnitude of the stiffness reduction.

From the results presented for the modified solid double wedge with a constant heat-transfer coefficient, it can be concluded that the flattening of the cross section reduces the maximum stiffness losses suffered by the unmodified wedge. On the other hand, slight degrees of blunting increase the torsional-stiffness reduction. It has been shown that, for both the blunted and the blunted and flattened wedge, ratios of tip thickness to midchord thickness up to approximately 0.20 exhibit an increase in torsional-stiffness reduction over that for the unblunted wedge. The percent variation in torsional-stiffness loss due to blunting seems to be independent of the magnitude of flattening of the cross section.

For the case of a constant value of heat-transfer coefficient the loss of torsional stiffness occurring in multiweb wings of light construction was substantially less than that of corresponding solid double-wedge wings.

The effect of a chordwise step transition in heat-transfer coefficient on the torsional-stiffness reduction of solid wings was found to depend on the magnitude of the resultant jump and upon the point of transition. In all the cases studied in this investigation, the influence of the step transition was to decrease the torsional-stiffness losses over those obtained with a uniform value of heat-transfer coefficient.

Langley Research Center,
National Aeronautics and Space Administration,
Langley Field, Va., October 14, 1958.

APPENDIX A

REDUCTION IN TORSIONAL STIFFNESS OF A MODIFIED DOUBLE WEDGE

The modified double-wedge section to be analyzed is shown in figure 1. For the purpose of this analysis, the assumptions mentioned in the section entitled "Basic Theory" are used. In addition, the heat-transfer coefficient is assumed constant along the chord. From equation (4) then, the temperature distribution which is symmetrical about the midchord can be written as

$$\left.\begin{aligned} \theta &= 1 - e^{-\lambda} && (0 \leqq x \leqq a) \\ \theta &= 1 - e^{\frac{-\lambda b}{a+b-x}} && \left(a \leqq x \leqq \frac{c}{2}\right) \end{aligned}\right\} \tag{A1}$$

With symmetry of temperature distribution about the midchord, the spanwise stress can be expressed by equation (11) where $\int_A \theta x \, dA = 0$ as

$$\frac{\sigma}{E\alpha \, \Delta T_{aw}} = \frac{2\int_0^{c/2} \theta t \, dx}{A_t} - \theta \tag{A2}$$

Substituting equation (A1) into equation (A2) and integrating yields

$$\left.\begin{aligned} \frac{\sigma}{E\alpha \, \Delta T_{aw}} &= e^{\frac{-\lambda b}{a+b-x}} + \frac{t_{max}}{A_t b}\left[-e^{-\lambda}\left(b^2 - \lambda b^2 + 2ba\right) + e^{\frac{-\lambda b}{L}}\left(L^2 - \lambda bL\right) + \lambda^2 b^2 F_o\right] && \left(a \leqq x \leqq \frac{c}{2}\right) \\ \frac{\sigma}{E\alpha \, \Delta T_{aw}} &= \frac{t_{max}}{A_t b}\left[-e^{-\lambda}\left(-\lambda b^2 + L^2\right) + e^{\frac{-\lambda b}{L}}\left(L^2 - \lambda bL\right) + \lambda^2 b^2 F_o\right] && (0 \leqq x \leqq a) \end{aligned}\right\} \tag{A3}$$

where $F_o = Ei(-\lambda) - Ei\left(\frac{-\lambda b}{L}\right)$, $L = a + b - \frac{c}{2}$, and $Ei(-\lambda)$ is the exponential integral function defined by

$$Ei(-\lambda) = -\int_{\lambda}^{\infty} \frac{e^{-\beta}}{\beta}\, d\beta \tag{A4}$$

If the expressions for stress in equation (A3) are substituted into equation (1) and the assumption is made that $J_o = 4I_{xx}$, the reduction in torsional stiffness becomes

$$\frac{GJ_{eff}}{GJ_o} = 1 + \frac{12}{G\left(t_{max}^3 b - Lt_{le}^3 + 4at_{max}^3\right)}\left[\int_0^a \sigma x^2 t_{max}\, dx + \int_a^{c/2} \sigma x^2 t_{max} \frac{(a + b - x)}{b}\, dx\right] \tag{A5}$$

where

$$J_o = \frac{1}{6}\left(t_{max}^3 b - Lt_{le}^3 + 4at_{max}^3\right) \tag{A6}$$

Integrating and simplifying the above equation results in the following expression:

$$\frac{GJ_{eff}}{GJ_o} = 1 - \frac{E\alpha}{G}\Delta T_{aw}\left(\frac{c}{t_{max}}\right)^2 \Phi$$

where

$$\Phi = \frac{12}{\left[b - L\left(\frac{t_{le}}{t_{max}}\right)^3 + 4a\right]c^2} \left\{\right\}$$

$$\left\{\ \right\} = e^{-\lambda}\left[\frac{(a+b)^2}{2}\, b(\lambda - 1) + \frac{b^2}{3}(a+b)\left(\lambda^2 - \lambda + 2\right) + \right.$$

$$\left.\frac{b^3}{24}\left(\lambda^3 - \lambda^2 + 2\lambda - 6\right)\right] + e^{\frac{-\lambda b}{L}}\left[\frac{L(a+b)^2}{2}\left(\frac{L}{b} - \lambda\right) - \right.$$

$$\left.\frac{L(a+b)}{3}\left(\frac{2L^2}{b} - \lambda L + \lambda^2 b\right) + \frac{L}{24}\left(\frac{6L^3}{b} - 2\lambda L^2 + \lambda^2 bL - \lambda^3 b^2\right)\right] +$$

$$F_o\lambda^2\, \frac{b}{24}\left[12(a+b)^2 + 8\lambda b(a+b) + \lambda^2 b^2\right] - \chi\left[(a+b)^2\left(\frac{b}{2} - \frac{L^2}{2b}\right) + \right.$$

$$\left.(a+b)\left(-\frac{2}{3}\, b^2 + \frac{2}{3}\,\frac{L^3}{b}\right) + \frac{b^3}{4} - \frac{L^4}{4b}\right] - \psi\left(\frac{a^3}{3}\right)$$

$$\chi = \frac{t_{max}}{A_t b}\left[-e^{-\lambda}\left(b^2 - \lambda b^2 + 2ba\right) + e^{\frac{-\lambda b}{L}}\left(L^2 - \lambda bL\right) + \lambda^2 b^2 F_o\right]$$

$$\psi = \frac{t_{max}}{A_t b}\left[-e^{-\lambda}\left(-\lambda b^2 + L^2\right) + e^{\frac{-\lambda b}{L}}\left(L^2 - \lambda bL\right) + \lambda^2 b^2 F_o\right]$$

APPENDIX B

REDUCTION IN TORSIONAL STIFFNESS OF A MULTIWEB WEDGE

The multiweb wing to be analyzed is shown in figure 6. The assumptions previously mentioned in the section entitled "Basic Theory" will be employed with the heat-transfer coefficient considered constant in the chordwise direction.

The temperature distribution of each skin of the multiweb is assumed to vary as that of a flat plate; hence,

$$\theta_s = 1 - e^{\frac{-\lambda}{2t_s/t_{max}}} \tag{B1}$$

The temperature distribution of the web material is assumed to vary as if the webs completely filled the interior of the multiweb and formed a solid double wedge. Thus,

$$\theta_w = 1 - e^{\frac{-\lambda}{t/t_{max}}} \tag{B2}$$

The average temperature in a typical bay of the multiweb can be written as

$$\theta = \frac{2b_w t_s \theta_s + t t_w \theta_w}{2b_w t_s + t t_w} \tag{B3}$$

In order to evaluate the spanwise stress at any point along the chord, the total web material is considered to vary continuously along the chord in proportion to the wing thickness. The expression for θ given in equation (B3) is then substituted into equation (11) for spanwise stress. Because of symmetry of temperature distribution about the midchord, $\int_A \theta x \, dA$ in equation (11) is equal to zero. Since

$dA = ct_s\left[1 + 2\left(\frac{2d}{c}\right)\frac{A_w}{A_s}\right]d\left(\frac{2d}{c}\right)$, by letting $\frac{2d}{c} = \xi$ the expression for spanwise stress becomes

$$\frac{\sigma}{E\alpha\,\Delta T_{aw}} = \frac{\int_0^1 \theta\left(1 + 2\xi\,\frac{A_w}{A_s}\right)d\xi}{\int_0^1 \left(1 + 2\xi\,\frac{A_w}{A_s}\right)d\xi} - \theta \tag{B4}$$

where

$$\frac{A_w}{A_s} = \frac{t_{max}t_w}{4b_w t_s}$$

Thus,

$$\frac{\sigma}{E\alpha\,\Delta T_{aw}} = \frac{1}{1 + \frac{A_w}{A_s}} \int_0^1 \left(\theta_s + 2\xi\theta_w\,\frac{A_w}{A_s}\right)d\xi - \theta \tag{B5}$$

Substitution of equation (B5) into equation (1) yields,

$$\frac{GJ_{eff}}{GJ_o} = 1 + \frac{2E\alpha}{GJ_o}\Delta T_{aw}\int_0^1\left[\frac{1}{1 + \frac{A_w}{A_s}}\int_0^1\left(\theta_s + 2\xi\theta_w\,\frac{A_w}{A_s}\right)d\xi - \theta\right]\left[\frac{c}{2}(1 - \xi)\right]^2 ct_s\left(1 + 2\xi\,\frac{A_w}{A_s}\right)d\xi \tag{B6}$$

The initial torsional stiffness of the multiweb GJ_o is derived by assuming that the webs are rigid in shear. Thus,

$$J_o = \frac{2}{3}\,ct_{max}^2 t_s \tag{B7}$$

By integrating and simplifying equation (B6), the reduction in torsional stiffness can be expressed as

$$\frac{GJ_{eff}}{GJ_o} = 1 - \frac{E\alpha}{G}\Delta T_{aw}\left(\frac{c}{t_{max}}\right)^2\Phi$$

where

$$\Phi = \frac{-1}{16}\left\{ 2e^{\frac{-\lambda}{2t_s/t_{max}}}\left(1 - \frac{A_s}{A_s + A_w}\right) - \right.$$

$$\frac{A_w}{A_s} e^{-\lambda}\left[\lambda^3 + 7\lambda^2 + 4\lambda + (1 - \lambda)\frac{2A_s}{A_s + A_w}\right] -$$

$$\left. \lambda^2 \frac{A_w}{A_s} F_1\left(\lambda^2 + 8\lambda + 10 - \frac{2A_s}{A_s + A_w}\right)\right\}$$

$$F_1 = -\int_{\lambda}^{\infty} \frac{e^{-\beta}}{\beta} d\beta = Ei(-\lambda)$$

APPENDIX C

EFFECT OF A VARIABLE HEAT-TRANSFER COEFFICIENT ON REDUCTION OF TORSIONAL STIFFNESS

In appendixes A and B the heat-transfer coefficient was assumed to be constant and the expressions for spanwise stress and torsional-stiffness reduction could be easily expressed in a closed form. However, when the heat-transfer coefficient is varied along the chord, a numerical integration procedure proves to be more expedient.

Consider any arbitrary symmetric cross section with a variable heat-transfer coefficient across the chord. If the cross section is first divided into N number of equally spaced elements, the expression for spanwise stress in equation (11) can be written as

$$\frac{\sigma_i}{E\alpha\left(\Delta T_{aw}\right)} = \frac{\sum_{i=1}^{N} \theta_i t_i}{\sum_{i=1}^{N} t_i} + \frac{\sum_{i=1}^{N} \theta_i x_i t_i}{\sum_{i=1}^{N} x_i^2 t_i} x_i - \theta_i \qquad \text{(C1)}$$

where

θ_i temperature of each element

t_i thickness of each element

x_i distance of each element from midchord

Substitution in equation (1) yields

$$\frac{GJ_{eff}}{GJ_o} = 1 + \frac{\delta}{GJ_o} \sum_{i=1}^{N} \sigma_i x_i^2 t_i \qquad \text{(C2)}$$

where δ is the width of an element. Let

$$Q_i = \frac{\sigma_i}{E\alpha\,\Delta T_{aw}} \tag{C3}$$

Then equation (C2) can be expressed as

$$\frac{GJ_{eff}}{GJ_o} = 1 - \frac{E\alpha}{G}\,\Delta T_{aw}\left(\frac{c}{t_{max}}\right)^2 \Phi$$

where

$$\Phi = \frac{\delta}{J_o}\sum_{i=1}^{N} x_i^2 t_i Q_i$$

REFERENCES

1. Budiansky, Bernard, and Mayers, J.: Influence of Aerodynamic Heating on the Effective Torsional Stiffness of Thin Wings. Jour. Aero. Sci., vol. 23, no. 12, Dec. 1956, pp. 1081-1093, 1108.

2. Kaye, Joseph: Survey of Friction Coefficients, Recovery Factors, and Heat-Transfer Coefficients for Supersonic Flow. Jour. Aero. Sci., vol. 21, no. 2, Feb. 1954, pp. 117-129.

3. Dryden, Hugh L., and Duberg, John E.: Aeroelastic Effects of Aerodynamic Heating. Proc. of the Fifth AGARD General Assembly (Canada), June 15-16, 1955, pp. 102-107.

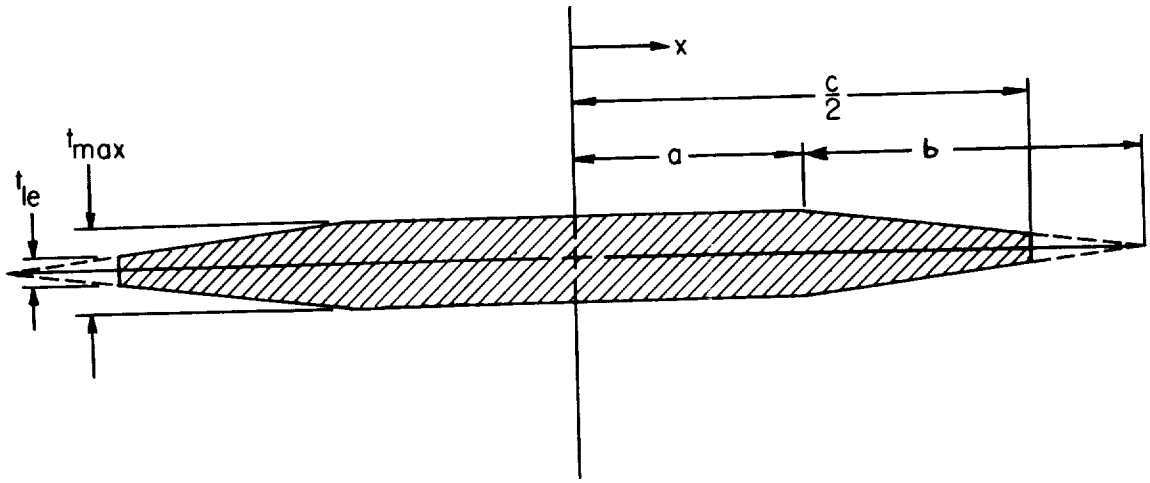

Figure 1.- Modified double-wedge wing.

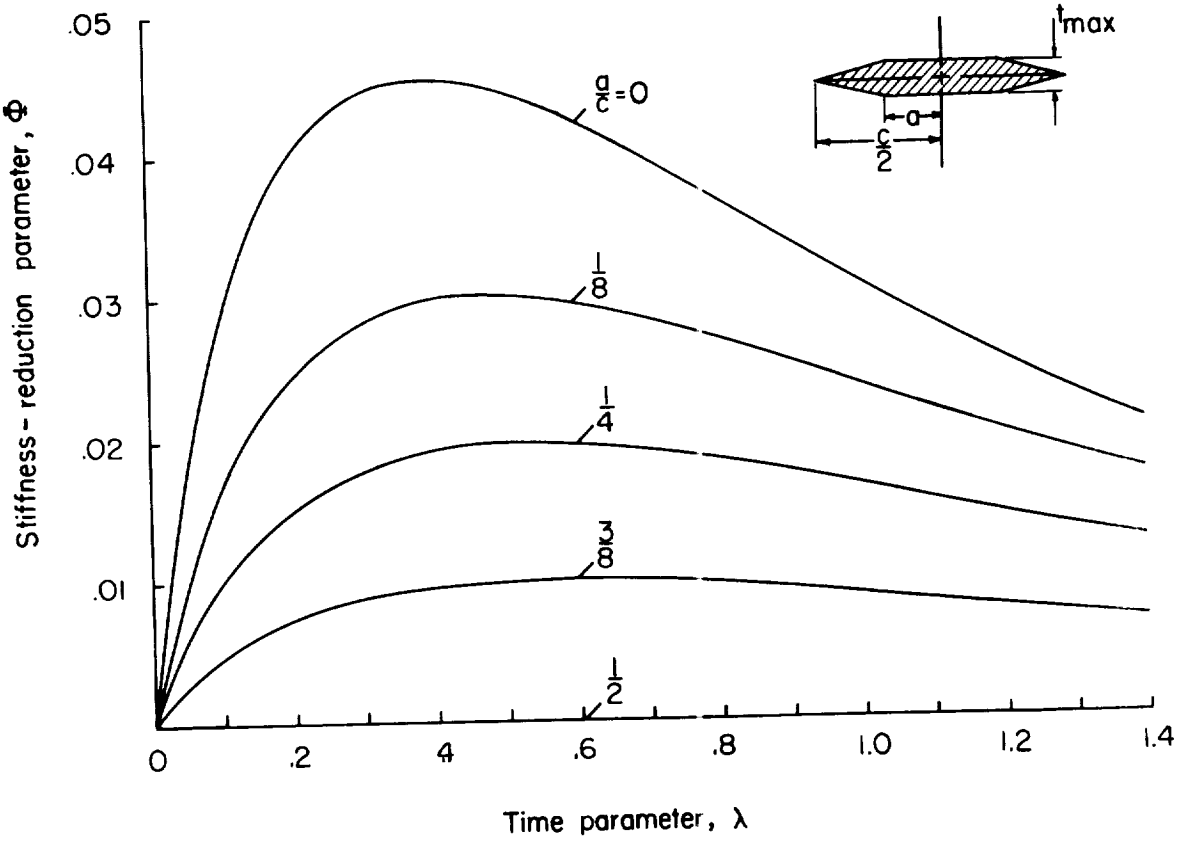

Figure 2.- Effect of flattening on torsional-stiffness reduction.

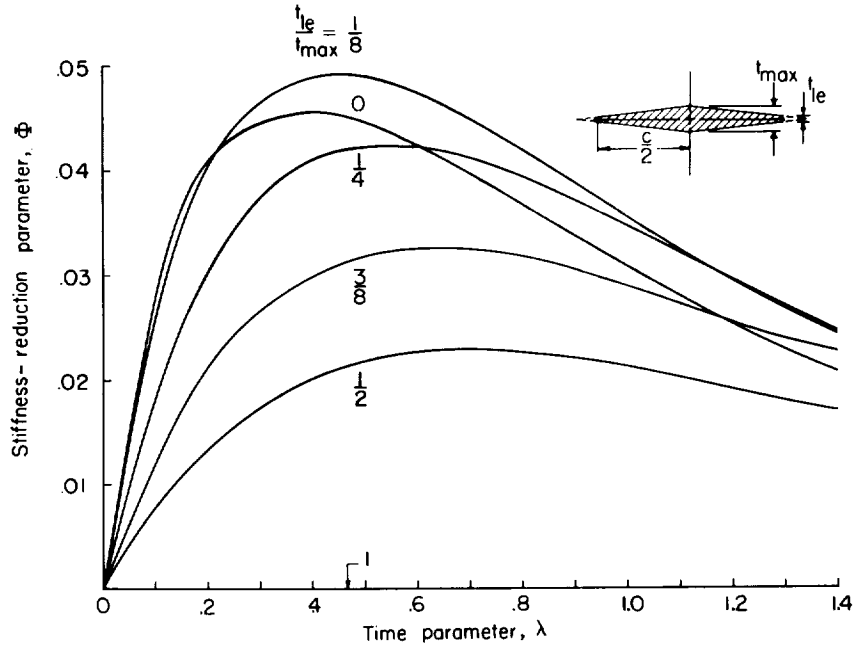

Figure 3.- Effect of blunting on torsional-stiffness reduction.

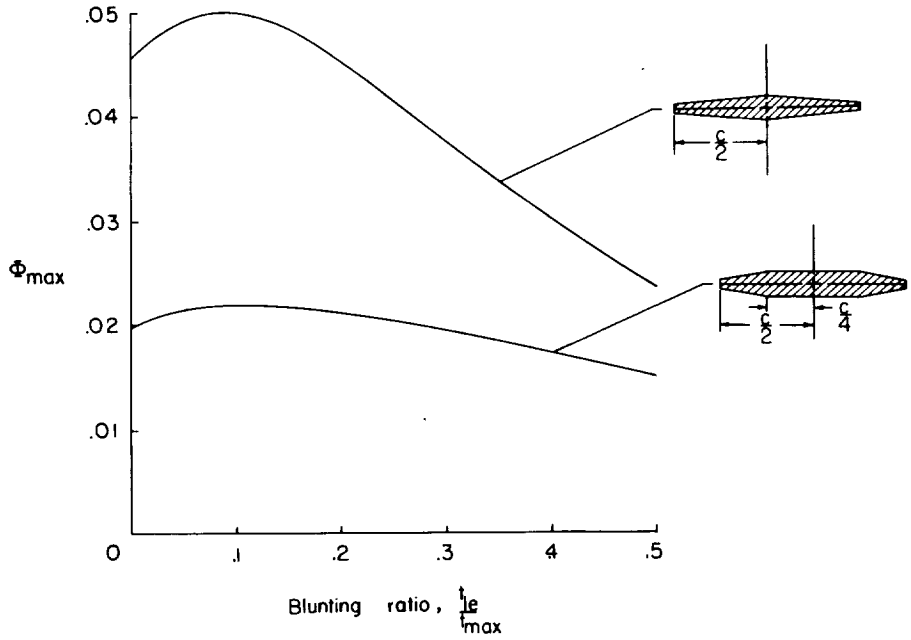

Figure 4.- Maximum stiffness reduction parameter Φ_{max} as a function of blunting ratio.

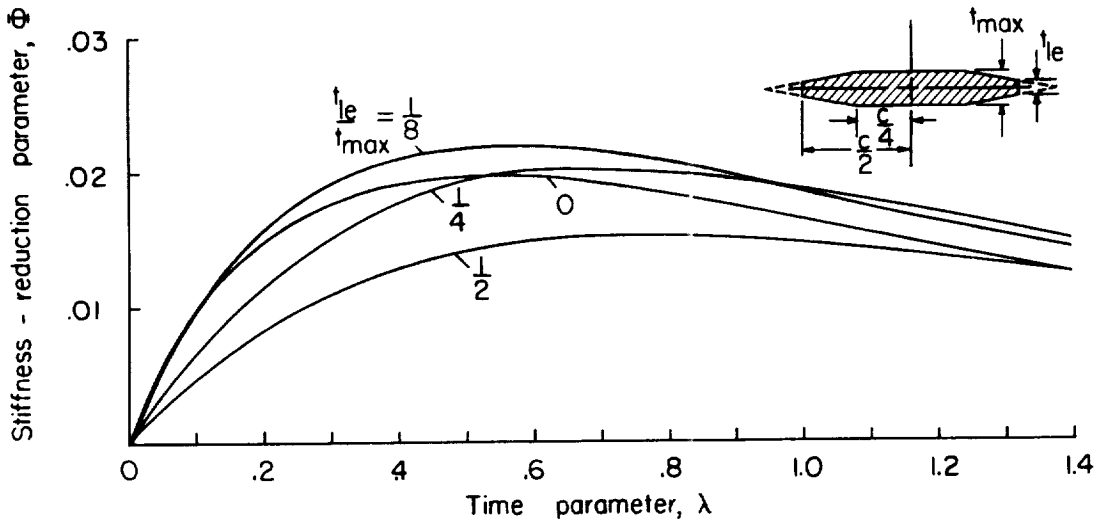

Figure 5.- Effect of combined blunting and flattening on torsional-stiffness reduction. $\frac{a}{c} = \frac{1}{4}$.

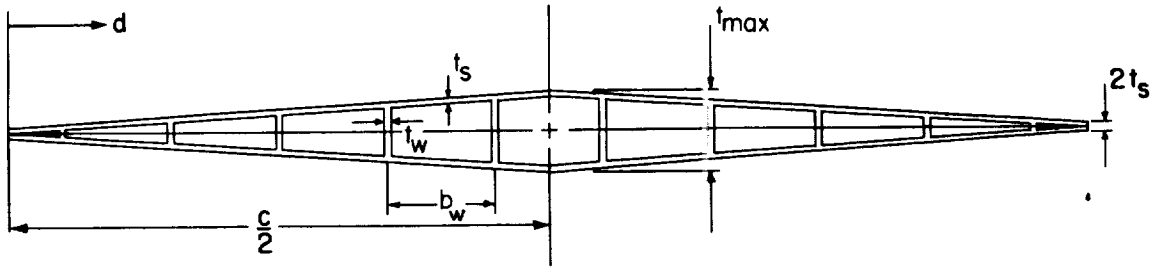

Figure 6.- Multiweb wing.

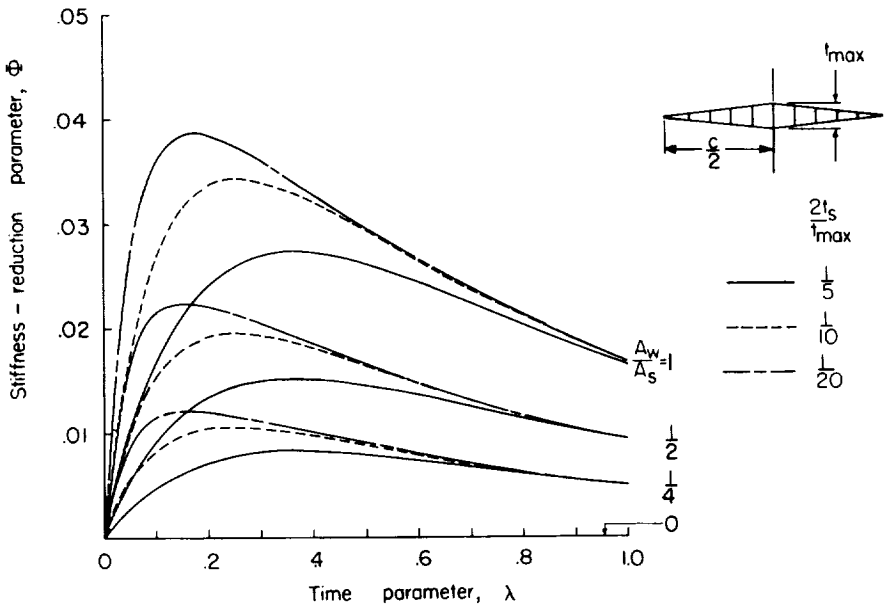

Figure 7.- Effect of area distribution of multiweb on torsional-stiffness reduction.

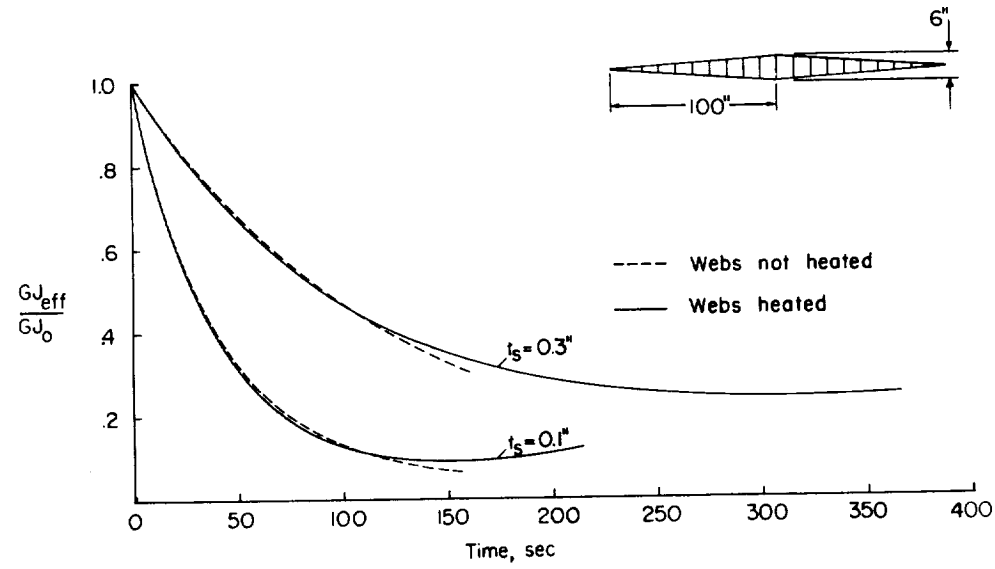

Figure 8.- Comparison of multiweb solutions. Thickness ratio, 3 percent; $M_o = 0.75$ - $M_f = 4.0$; altitude, 50,000 feet; $\frac{A_w}{A_s} = 0.35$.

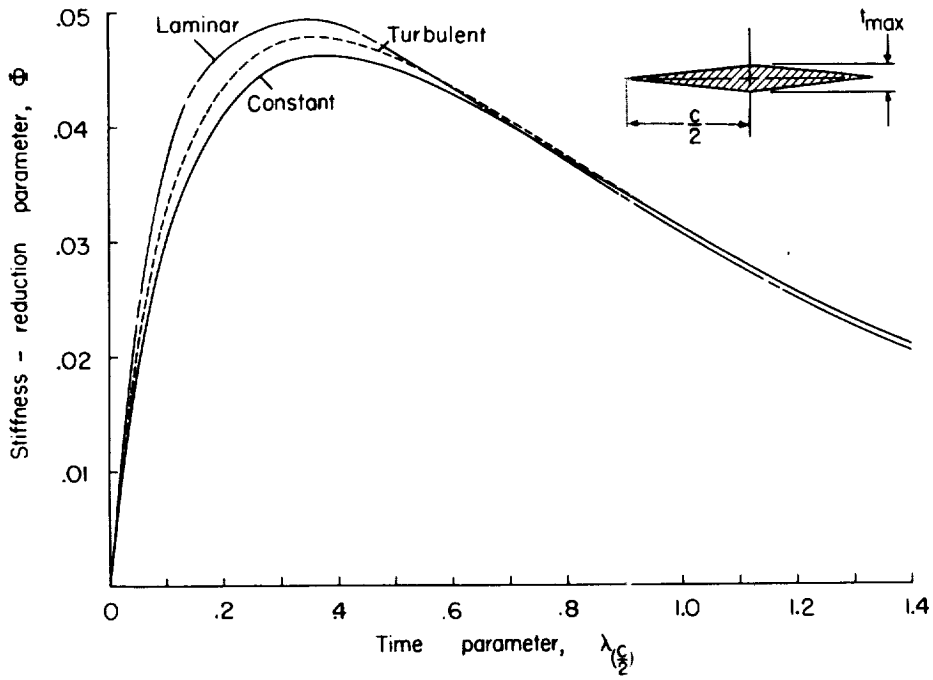

Figure 9.- Effect of a variable heat-transfer coefficient on torsional-stiffness reduction of a solid double-wedge wing.

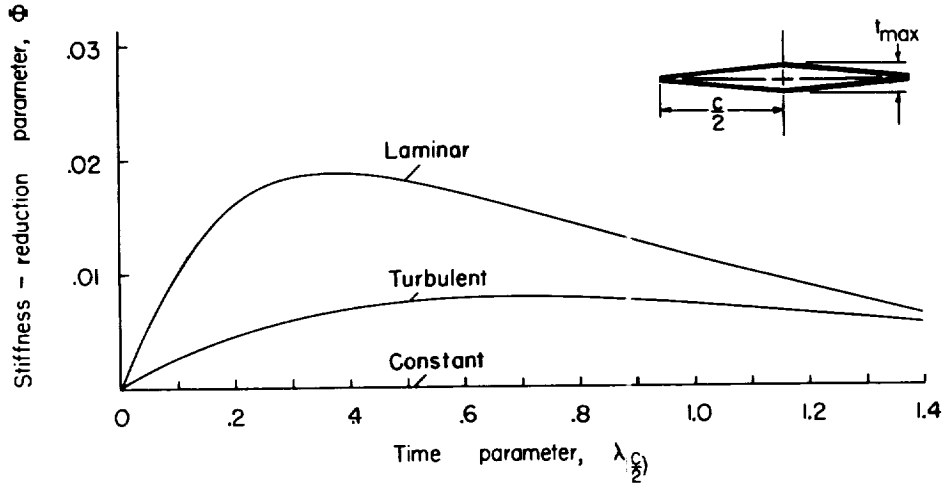

Figure 10.- Effect of a variable heat-transfer coefficient on torsional-stiffness reduction of a hollow double-wedge wing.

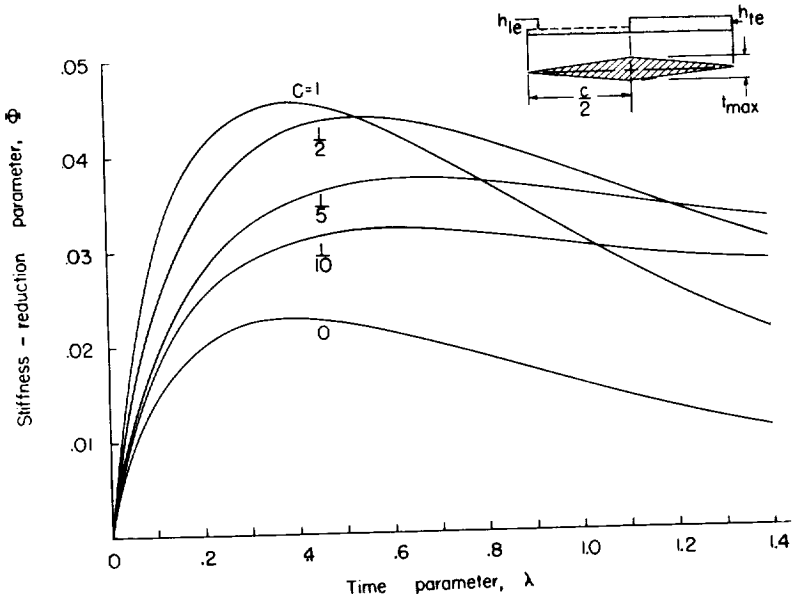

Figure 11.- Effect of transition at midchord on torsional-stiffness reduction. $\frac{h_{le}}{h_{te}} = C$.

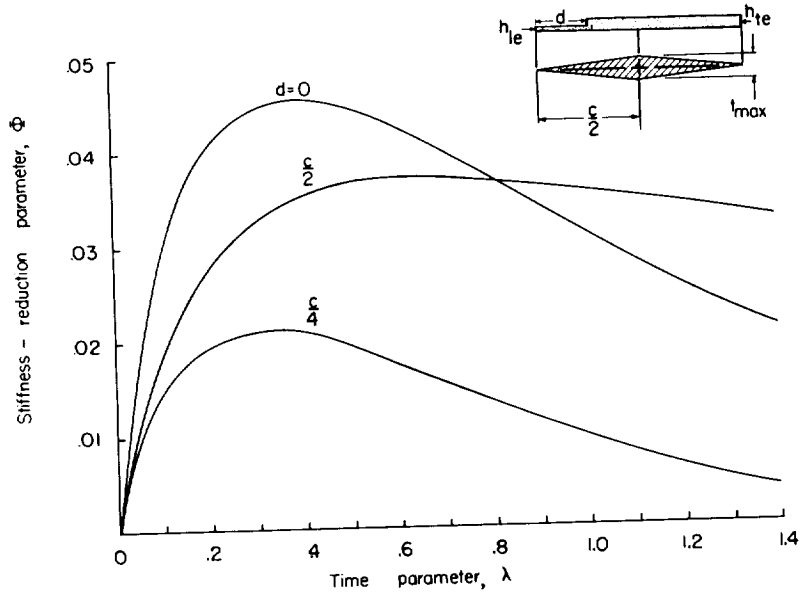

Figure 12.- Effect of varying transition-point on torsional-stiffness reduction for $\frac{h_{le}}{h_{te}} = \frac{1}{5}$.

NASA - Langley Field, Va. L-148